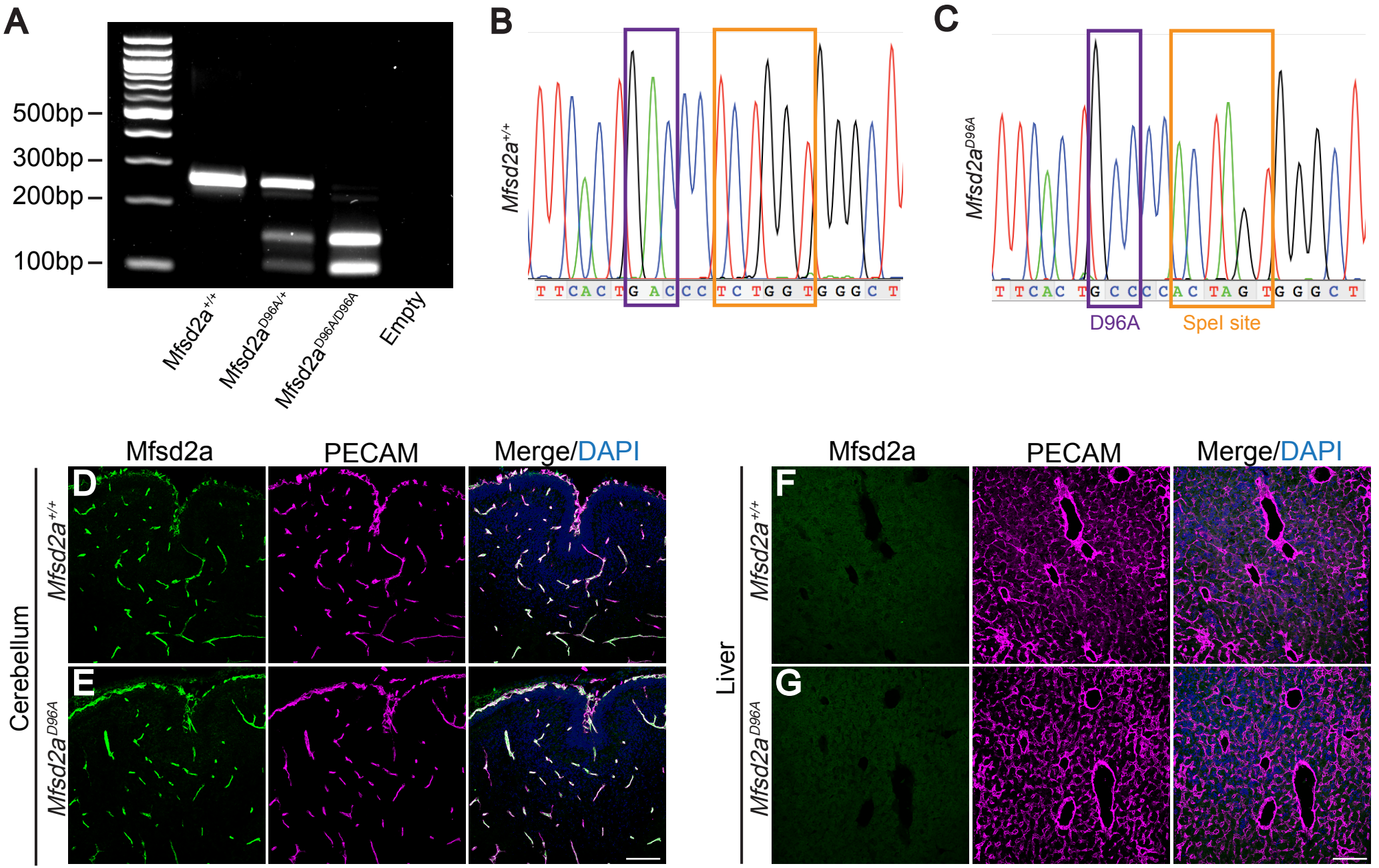
A
500bp
300bp
200bp
100bp
Mfsd2a+/+
Mfsd2aD96A/+
Mfsd2aD96A/D96A
Empty
B
Mfsd2a+/+
T T C A C T G A C C C T C T G G T G G G C T
C
Mfsd2aD96A
T T C A C T G C C C C A C T A G T G G G C T
D96A
SpeI site
Mfsd2a
PECAM
Merge/DAPI
Cerebellum
D
Mfsd2a+/+
E
Mfsd2aD96A
Liver
F
Mfsd2a+/+
G
Mfsd2aD96A

Figure S1

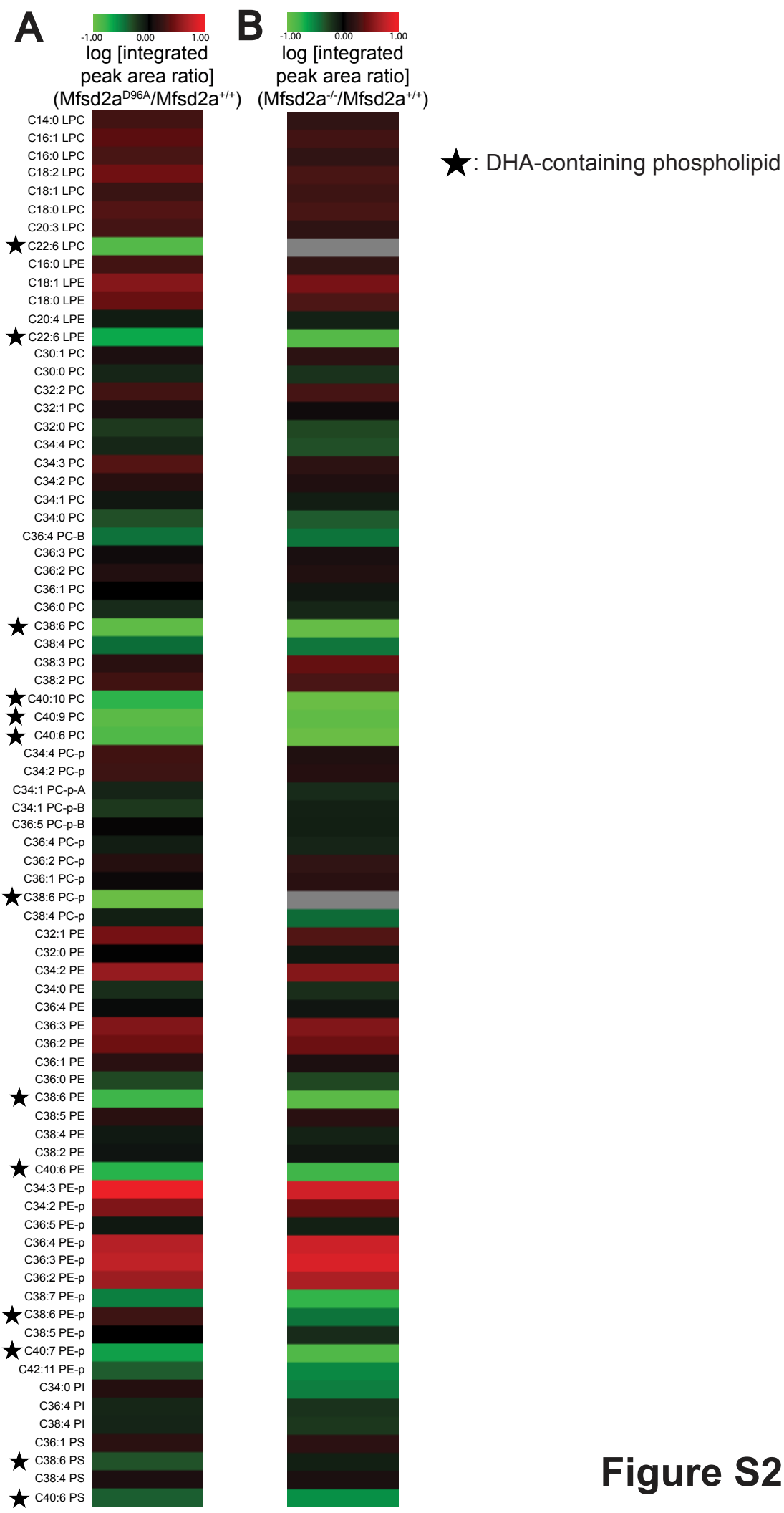
A
-1.00
0.00
1.00
log [integrated peak area ratio] (Mfsd2a^{D96A}/Mfsd2a$^{+/+}$)
B
-1.00
0.00
1.00
log [integrated peak area ratio] (Mfsd2a$^{-/-}$/Mfsd2a$^{+/+}$)
★: DHA-containing phospholipid
C14:0 LPC
C16:1 LPC
C16:0 LPC
C18:2 LPC
C18:1 LPC
C18:0 LPC
C20:3 LPC
★C22:6 LPC
C16:0 LPE
C18:1 LPE
C18:0 LPE
C20:4 LPE
★C22:6 LPE
C30:1 PC
C30:0 PC
C32:2 PC
C32:1 PC
C32:0 PC
C34:4 PC
C34:3 PC
C34:2 PC
C34:1 PC
C34:0 PC
C36:4 PC-B
C36:3 PC
C36:2 PC
C36:1 PC
C36:0 PC
★C38:6 PC
C38:4 PC
C38:3 PC
C38:2 PC
★C40:10 PC
★C40:9 PC
★C40:6 PC
C34:4 PC-p
C34:2 PC-p
C34:1 PC-p-A
C34:1 PC-p-B
C36:5 PC-p-B
C36:4 PC-p
C36:2 PC-p
C36:1 PC-p
★C38:6 PC-p
C38:4 PC-p
C32:1 PE
C32:0 PE
C34:2 PE
C34:0 PE
C36:4 PE
C36:3 PE
C36:2 PE
C36:1 PE
C36:0 PE
★C38:6 PE
C38:5 PE
C38:4 PE
C38:2 PE
★C40:6 PE
C34:3 PE-p
C34:2 PE-p
C36:5 PE-p
C36:4 PE-p
C36:3 PE-p
C36:2 PE-p
C38:7 PE-p
★C38:6 PE-p
C38:5 PE-p
★C40:7 PE-p
C42:11 PE-p
C34:0 PI
C36:4 PI
C38:4 PI
C36:1 PS
★C38:6 PS
C38:4 PS
★C40:6 PS

Figure S2

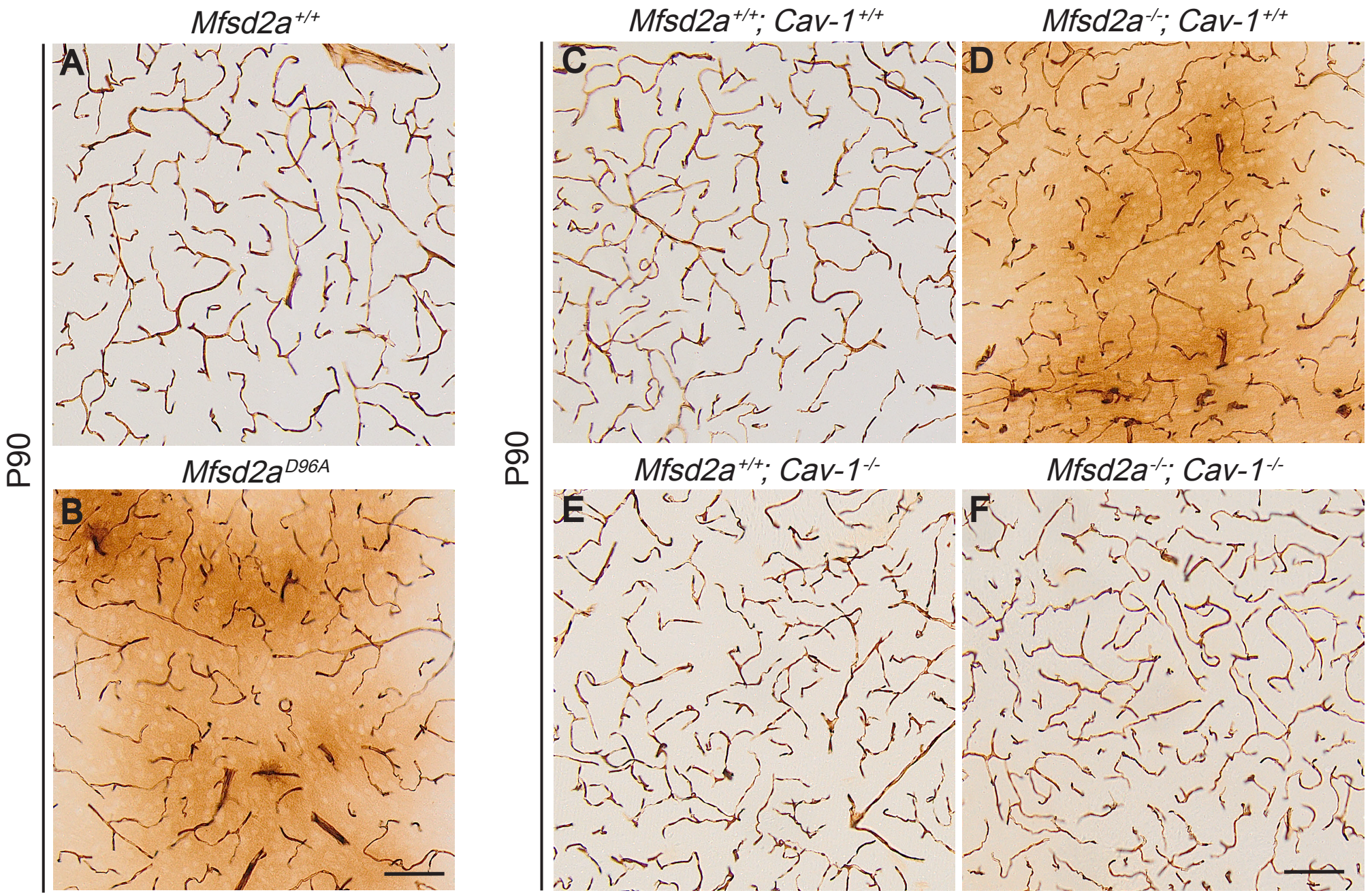
Mfsd2a+/+
A
Mfsd2aD96A
B
P90
Mfsd2a+/+; Cav-1+/+
C
Mfsd2a-/-; Cav-1+/+
D
Mfsd2a+/+; Cav-1-/-
E
Mfsd2a-/-; Cav-1-/-
F
P90

Figure S3

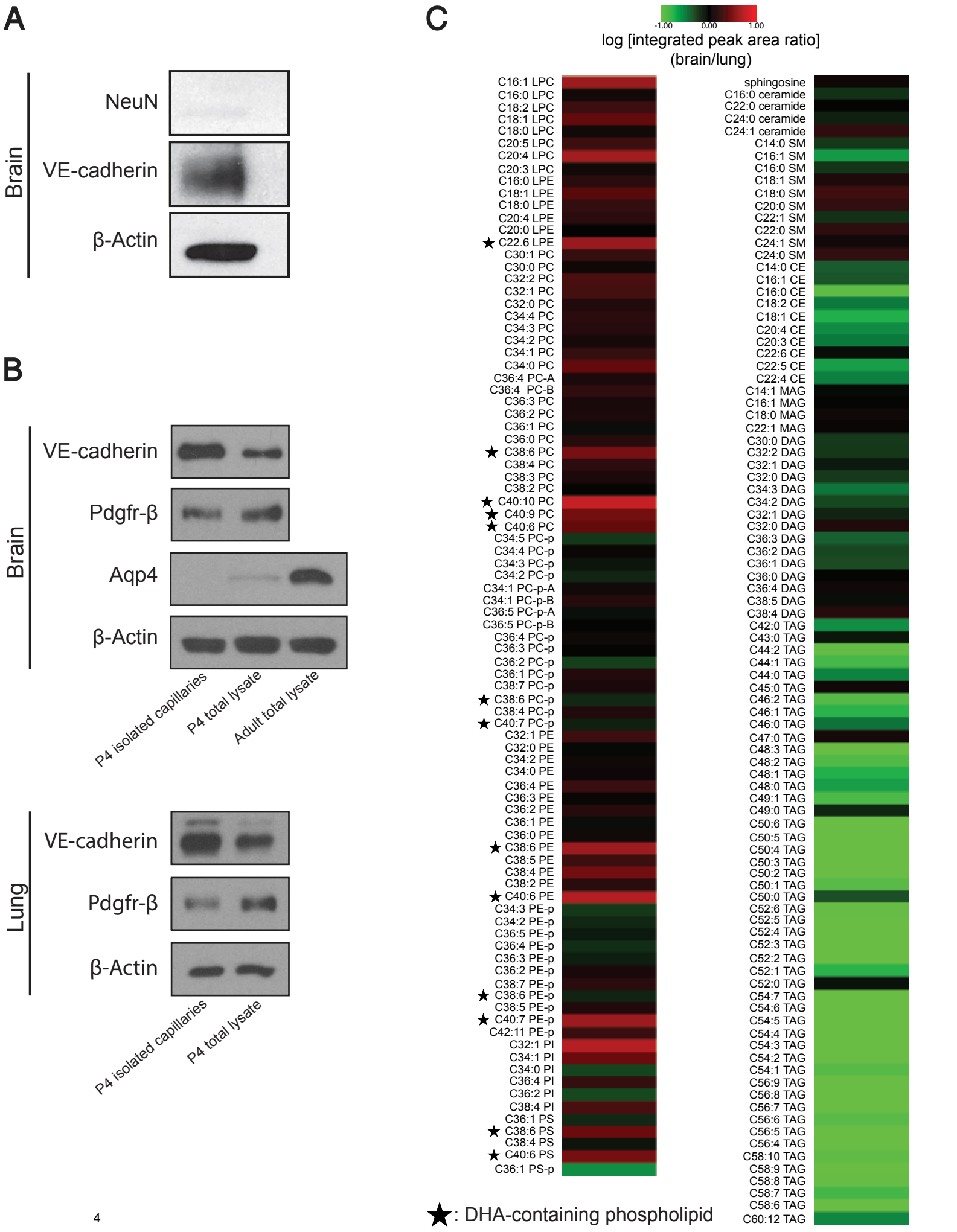
A
Brain
NeuN
VE-cadherin
β-Actin
B
Brain
VE-cadherin
Pdgfr-β
Aqp4
β-Actin
P4 isolated capillaries
P4 total lysate
Adult total lysate
Lung
VE-cadherin
Pdgfr-β
β-Actin
P4 isolated capillaries
P4 total lysate
C
-1.00
0.00
1.00
log [integrated peak area ratio]
(brain/lung)
C16:1 LPC
C16:0 LPC
C18:2 LPC
C18:1 LPC
C18:0 LPC
C20:5 LPC
C20:4 LPC
C20:3 LPC
C16:0 LPE
C18:1 LPE
C18:0 LPE
C20:4 LPE
C20:0 LPE
★ C22.6 LPE
C30:1 PC
C30:0 PC
C32:2 PC
C32:1 PC
C32:0 PC
C34:4 PC
C34:3 PC
C34:2 PC
C34:1 PC
C34:0 PC
C36:4 PC-A
C36:4 PC-B
C36:3 PC
C36:2 PC
C36:1 PC
C36:0 PC
★ C38:6 PC
C38:4 PC
C38:3 PC
C38:2 PC
★ C40:10 PC
★ C40:9 PC
★ C40:6 PC
C34:5 PC-p
C34:4 PC-p
C34:3 PC-p
C34:2 PC-p
C34:1 PC-p-A
C34:1 PC-p-B
C36:5 PC-p-A
C36:5 PC-p-B
C36:4 PC-p
C36:3 PC-p
C36:2 PC-p
C36:1 PC-p
C38:7 PC-p
★ C38:6 PC-p
C38:4 PC-p
★ C40:7 PC-p
C32:1 PE
C32:0 PE
C34:2 PE
C34:0 PE
C36:4 PE
C36:3 PE
C36:2 PE
C36:1 PE
C36:0 PE
★ C38:6 PE
C38:5 PE
C38:4 PE
C38:2 PE
★ C40:6 PE
C34:3 PE-p
C34:2 PE-p
C36:5 PE-p
C36:4 PE-p
C36:3 PE-p
C36:2 PE-p
C38:7 PE-p
★ C38:6 PE-p
C38:5 PE-p
★ C40:7 PE-p
C42:11 PE-p
C32:1 PI
C34:1 PI
C34:0 PI
C36:4 PI
C36:2 PI
C38:4 PI
C36:1 PS
★ C38:6 PS
C38:4 PS
★ C40:6 PS
C36:1 PS-p
sphingosine
C16:0 ceramide
C22:0 ceramide
C24:0 ceramide
C24:1 ceramide
C14:0 SM
C16:1 SM
C16:0 SM
C18:1 SM
C18:0 SM
C20:0 SM
C22:1 SM
C22:0 SM
C24:1 SM
C24:0 SM
C14:0 CE
C16:1 CE
C16:0 CE
C18:2 CE
C18:1 CE
C20:4 CE
C20:3 CE
C22:6 CE
C22:5 CE
C22:4 CE
C14:1 MAG
C16:1 MAG
C18:0 MAG
C22:1 MAG
C30:0 DAG
C32:2 DAG
C32:1 DAG
C32:0 DAG
C34:3 DAG
C34:2 DAG
C32:1 DAG
C32:0 DAG
C36:3 DAG
C36:2 DAG
C36:1 DAG
C36:0 DAG
C36:4 DAG
C38:5 DAG
C38:4 DAG
C42:0 TAG
C43:0 TAG
C44:2 TAG
C44:1 TAG
C44:0 TAG
C45:0 TAG
C46:2 TAG
C46:1 TAG
C46:0 TAG
C47:0 TAG
C48:3 TAG
C48:2 TAG
C48:1 TAG
C48:0 TAG
C49:1 TAG
C49:0 TAG
C50:6 TAG
C50:5 TAG
C50:4 TAG
C50:3 TAG
C50:2 TAG
C50:1 TAG
C50:0 TAG
C52:6 TAG
C52:5 TAG
C52:4 TAG
C52:3 TAG
C52:2 TAG
C52:1 TAG
C52:0 TAG
C54:7 TAG
C54:6 TAG
C54:5 TAG
C54:4 TAG
C54:3 TAG
C54:2 TAG
C54:1 TAG
C56:9 TAG
C56:8 TAG
C56:7 TAG
C56:6 TAG
C56:5 TAG
C56:4 TAG
C58:10 TAG
C58:9 TAG
C58:8 TAG
C58:7 TAG
C58:6 TAG
C60:12 TAG
★: DHA-containing phospholipid

Figure S4

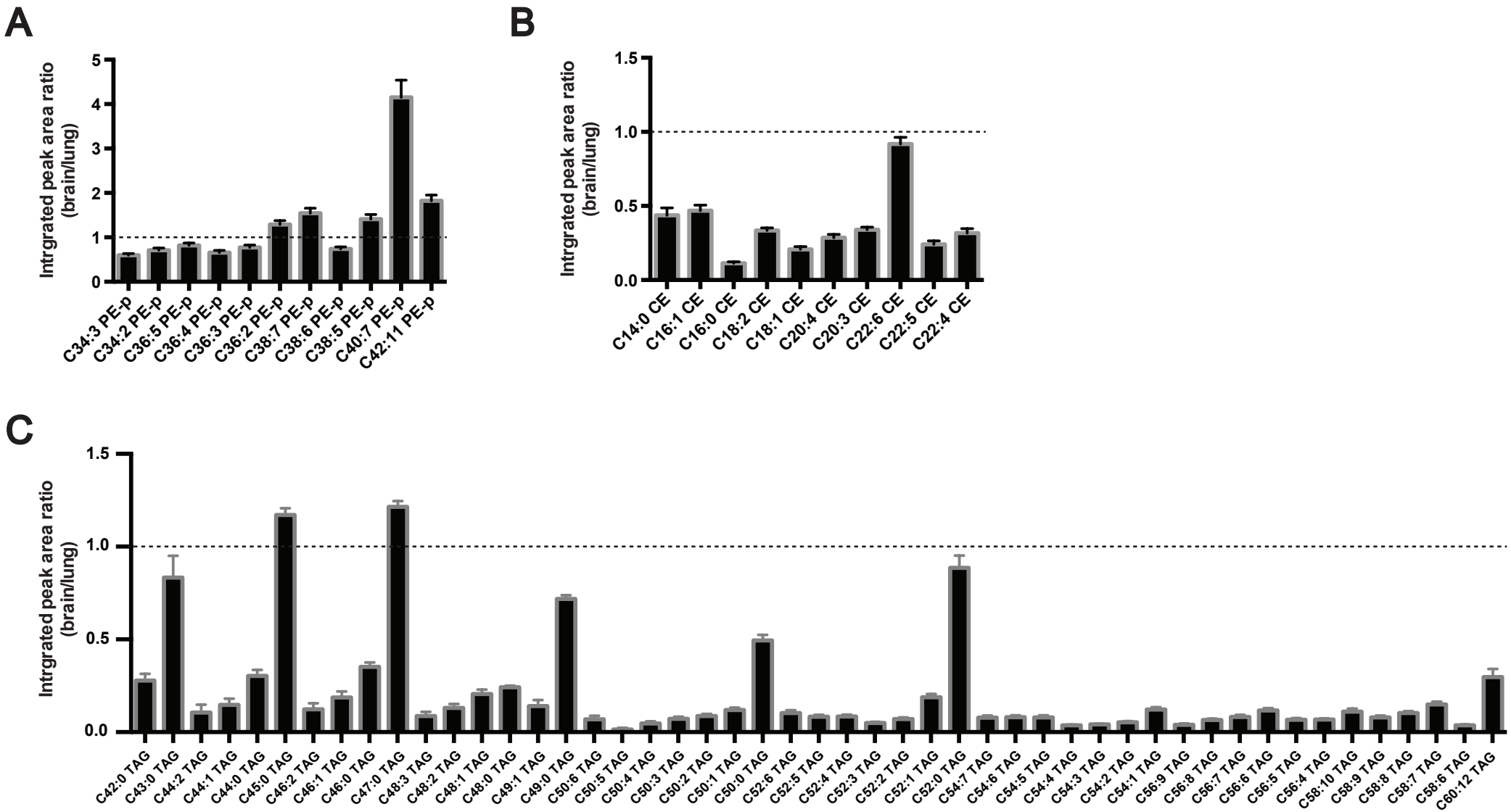
A
Intrgrated peak area ratio (brain/lung)
5
4
3
2
1
0
C34:3 PE-p
C34:2 PE-p
C36:5 PE-p
C36:4 PE-p
C36:3 PE-p
C36:2 PE-p
C38:7 PE-p
C38:6 PE-p
C38:5 PE-p
C40:7 PE-p
C42:11 PE-p
B
Intrgrated peak area ratio (brain/lung)
1.5
1.0
0.5
0.0
C14:0 CE
C16:1 CE
C16:0 CE
C18:2 CE
C18:1 CE
C20:4 CE
C20:3 CE
C22:6 CE
C22:5 CE
C22:4 CE
C
Intrgrated peak area ratio (brain/lung)
1.5
1.0
0.5
0.0
C42:0 TAG
C43:0 TAG
C44:2 TAG
C44:1 TAG
C44:0 TAG
C45:0 TAG
C46:2 TAG
C46:1 TAG
C46:0 TAG
C47:0 TAG
C48:3 TAG
C48:2 TAG
C48:1 TAG
C48:0 TAG
C49:1 TAG
C49:0 TAG
C50:6 TAG
C50:5 TAG
C50:4 TAG
C50:3 TAG
C50:2 TAG
C50:1 TAG
C50:0 TAG
C52:6 TAG
C52:5 TAG
C52:4 TAG
C52:3 TAG
C52:2 TAG
C52:1 TAG
C52:0 TAG
C54:7 TAG
C54:6 TAG
C54:5 TAG
C54:4 TAG
C54:3 TAG
C54:2 TAG
C54:1 TAG
C56:9 TAG
C56:8 TAG
C56:7 TAG
C56:6 TAG
C56:5 TAG
C56:4 TAG
C58:10 TAG
C58:9 TAG
C58:8 TAG
C58:7 TAG
C58:6 TAG
C60:12 TAG

Figure S5

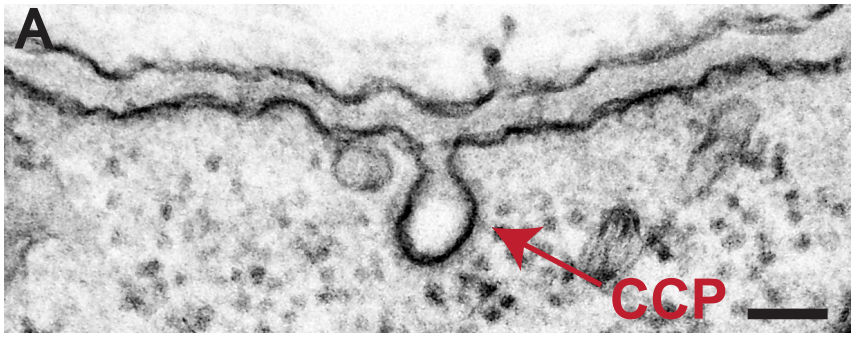
A
CCP

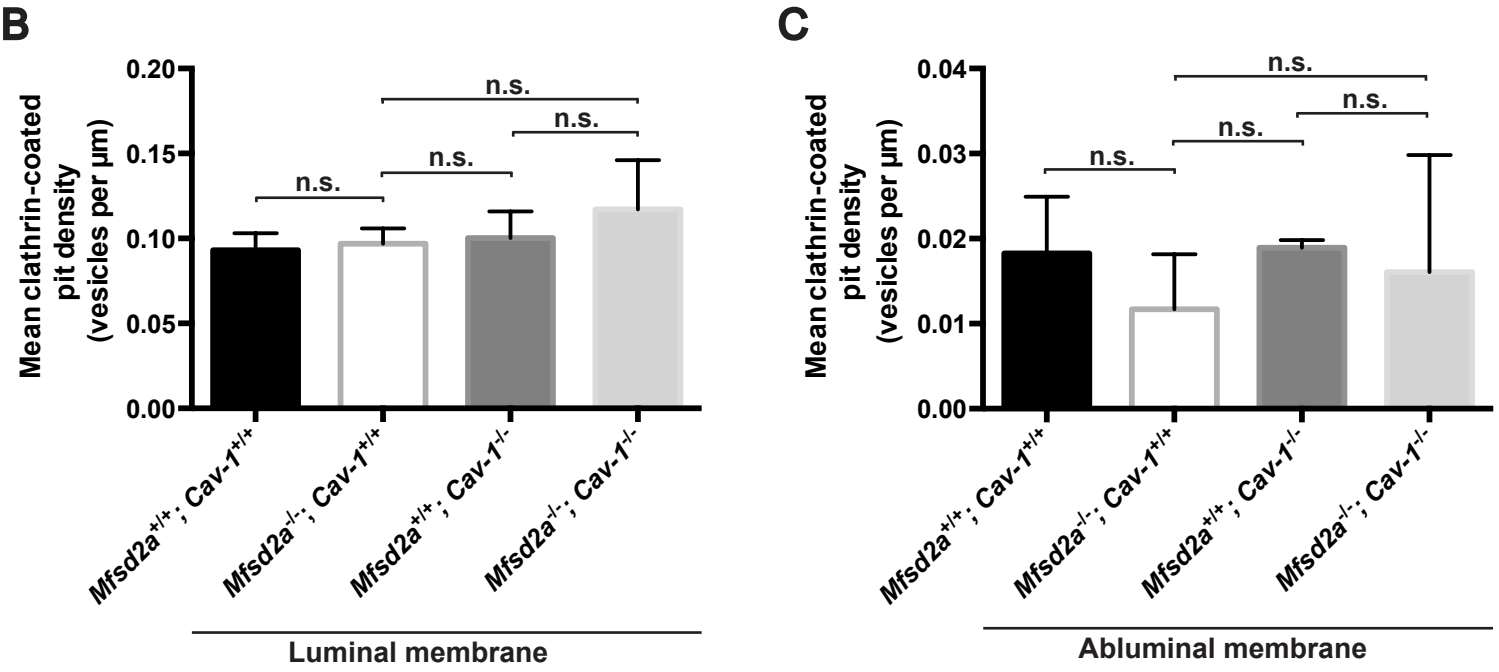
B
Mean clathrin-coated pit density (vesicles per µm)
0.20
0.15
0.10
0.05
0.00
n.s.
n.s.
n.s.
n.s.
Mfsd2a+/+; Cav-1+/+
Mfsd2a-/-; Cav-1+/+
Mfsd2a+/+; Cav-1-/-
Mfsd2a-/-; Cav-1-/-
Luminal membrane
C
Mean clathrin-coated pit density (vesicles per µm)
0.04
0.03
0.02
0.01
0.00
n.s.
n.s.
n.s.
n.s.
Mfsd2a+/+; Cav-1+/+
Mfsd2a-/-; Cav-1+/+
Mfsd2a+/+; Cav-1-/-
Mfsd2a-/-; Cav-1-/-
Abluminal membrane

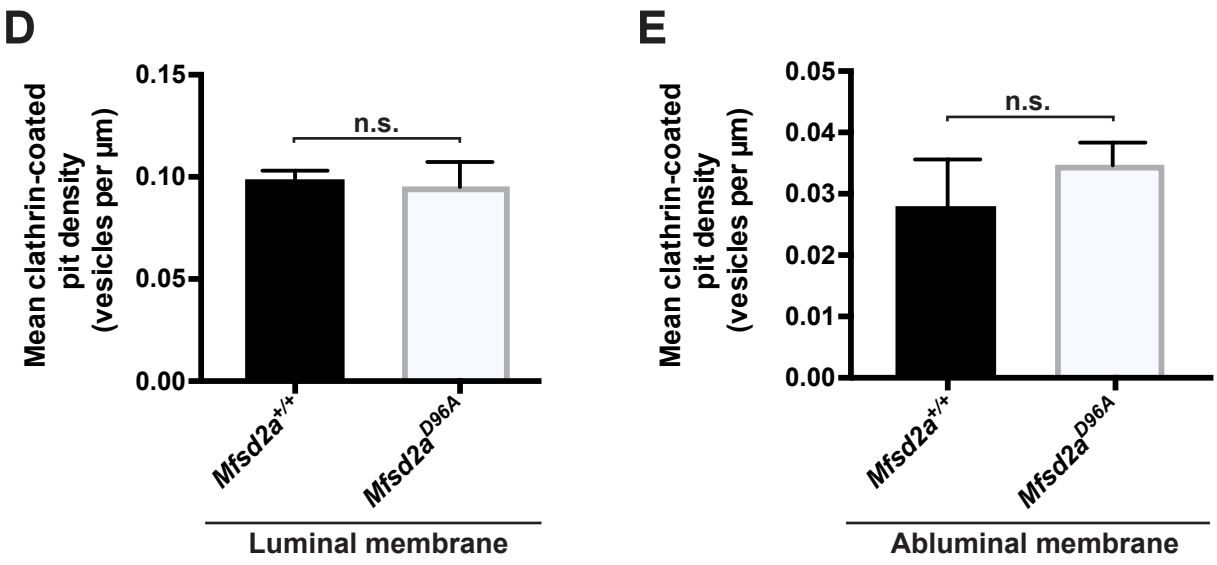
D
Mean clathrin-coated pit density (vesicles per µm)
0.15
0.10
0.05
0.00
n.s.
Mfsd2a+/+
Mfsd2aD96A
Luminal membrane
E
Mean clathrin-coated pit density (vesicles per µm)
0.05
0.04
0.03
0.02
0.01
0.00
n.s.
Mfsd2a+/+
Mfsd2aD96A
Abluminal membrane

Figure S6

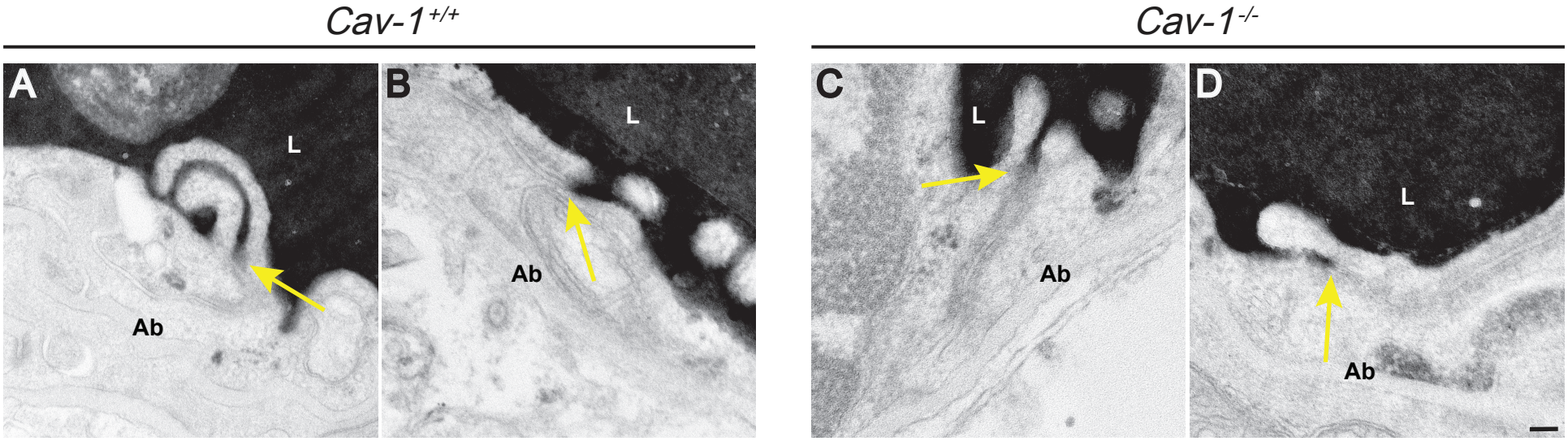

Figure S7

Table S1

Metabolite	*Mfds2a*$^{+/+}$ Average (Integrated Peak Area)	*Mfds2a*^{D96A} Average (Integrated Peak Area)	Ratio *Mfds2a*^{D96A} : *Mfds2a*$^{+/+}$	p-value
C14:0 LPC	1559496	3046444	1.95	8.756E-05
C16:1 LPC	4252239	10056141	2.36	1.644E-07
C16:0 LPC	42087015	87182505	2.07	8.515E-05
C18:2 LPC	427454	1215604	2.84	0.0001
C18:1 LPC	6187399	11368348	1.84	2.111-07
C18:0 LPC	14977640	33607528	2.24	0.0004
C20:5 LPC	119254	207843	1.74	0.0071
C20:3 LPC	20321741	40620082	2.00	0.0001
C22:6 LPC	1153049	149263	0.13	4.547E-05
C16:0 LPE	2265887	4446666	1.96	0.0003
C18:1 LPE	934537	3187066	3.41	6.259E-07
C18:0 LPE	4743681	12657290	2.67	3.071E-05
C20:4 LPE	1249279	1045681	0.84	0.0359
C20:0 LPE	27931258	28046298	1.00	0.8435
C22:6 LPE	3009190	653912	0.22	7.566E-08
C30:1 PC	73818365	92237435	1.25	0.0153
C30:0 PC	1230078651	907228758	0.74	9.317E-05
C32:2 PC	254992058	494068990	1.94	5.656E-09
C32:1 PC	3000823942	3725038390	1.24	5.254E-05
C32:0 PC	3442716003	2044796301	0.59	7.478E-09
C34:4 PC	25245719	18193882	0.72	0.0001
C34:3 PC	64300362	145254788	2.26	3.914E-09
C34:2 PC	808115610	1160847723	1.44	2.997E-07
C34:1 PC	4333465246	3822126337	0.88	0.0001
C34:0 PC	532407446	261625969	0.49	1.469E-07
C36:4 PC-B	801646431	286908040	0.36	4.852E-07
C36:3 PC	156443801	175312933	1.12	0.0615
C36:2 PC	556261799	750755225	1.35	1.997E-05
C36:1 PC	547027164	547419430	1.00	0.9759
C36:0 PC	4138838	2812945	0.68	2.605E-06
C38:6 PC	491475841	56443724	0.11	3.393E-06
C38:4 PC	511872806	192419142	0.38	1.124E-09
C38:3 PC	37248063	55524451	1.49	4.295E-05
C38:2 PC	17177409	33153444	1.93	3.553E-07
C40:10 PC	13966079	2501377	0.18	7.722E-07
C40:9 PC	107579685	12946028	0.12	5.655E-07
C40:6 PC	185170888	25286613	0.14	1.632E-06
C34:5 PC-p	332177	391995	1.18	0.1582
C34:4 PC-p	1904900	3662084	1.92	1.631E-06
C34:3 PC-p	10525921	8733773	0.83	0.0009
C34:2 PC-p	3177838	6030576	1.90	0.0001
C34:1 PC-p -A	122516521	91599159	0.75	4.105E-05
C34:1 PC-p -B	822793	495574.2286	0.60	1.941E-06
C36:5 PC-p -B	4807912	5065924	1.05	0.2977
C36:4 PC-p	31516527	25968322	0.82	0.0003
C36:1 PC-p	2680426	2910359	1.09	0.1829
C38:6 PC-p	5943363	284871	0.05	0.0303
C38:4 PC-p	2172152	1749591	0.81	0.0138
C32:1 PE	8803907	26019517	2.96	3.742E-07
C32:0 PE	4804769	4727672	0.98	0.7759
C34:2 PE	18062523	70143304	3.88	6.204E-07
C34:0 PE	44030552	29096804	0.66	5.193E-06
C36:4 PE	87599065	84082064	0.96	0.4224

C36:3 PE	9665857	31778107	3.29	7.825E-08
C36:2 PE	34848601	96863825	2.78	6.421E-09
C36:1 PE	34134806	50027413	1.47	4.922E-07
C36:0 PE	17888202	9270952	0.52	7.903E-07
C38:6 PE	271784659	44552562	0.16	1.155E-06
C38:5 PE	67699189	99853443	1.47	0.0002
C38:4 PE	397298387	340843607	0.86	0.0015
C38:2 PE	25882702	23720016	0.92	0.0120
C40:6 PE	293102114	53937239	0.18	9.580E-07
C34:3 PE-p	2551676	22608314	8.86	1.024E-06
C34:2 PE-p	25475888	81667144	3.21	8.405E-08
C36:5 PE-p	46891502	41130600	0.88	0.0097
C36:4 PE-p	3567798	18699008	5.24	3.567E-07
C36:3 PE-p	7717570	44173575	5.72	7.053E-07
C36:2 PE-p	6477014	26695284	4.12	7.604E-07
C36:1 PE-p	1315463	5551408	4.22	2.810E-06
C38:7 PE-p	179954458	57607450	0.32	1.456E-10
C38:6 PE-p	26029794	48682078	1.87	0.0002
C38:5 PE-p	45349533	45296805	1.00	0.9740
C40:7 PE-p	146241617	34650609	0.24	8.083E-08
C42:11 PE-p	9366396	4098394	0.44	1.745E-06
C32:1 PI	3853260	1813039	0.47	2.750E-07
C34:1 PI	67528398	26737473	0.40	3.464E-08
C34:0 PI	2499614	3425595	1.37	0.0235
C36:4 PI	2907327	2117484	0.73	0.0002
C38:4 PI	13538544	10170610	0.75	0.0006
C36:1 PS	6938482	10597772	1.53	1.118E-06
C38:6 PS	8449033	4019122	0.48	1.800E-07
C38:4 PS	19772756	24431554	1.24	0.0011
C40:6 PS	128490473	55023803	0.43	4.586E-09
sphingosine	359191	694876	1.93	0.0240
C14:0 SM	593028	1057588	1.78	4.062E-05
C16:1 SM	1684781	2314573	1.37	0.0027
C16:0 SM	43831912	52786212	1.20	0.0128
C18:1 SM	24475979	26905114	1.09	0.0674
C18:0 SM	180983246	190229406	1.05	0.3547
C20:0 SM	9441323	9984594	1.05	0.2661
C22:1 SM	1597303	2123389	1.32	0.0004
C22:0 SM	7222196	7454390	1.03	0.5349
C24:1 SM	19760089	24856191	1.25	0.0011
C24:0 SM	4927540	4938167	1.00	0.9690
C16:1 CE	309778	1123250	3.62	0.0012
C16:0 CE	194289	586732	3.01	0.0008
C18:2 CE	762391	1383177	1.81	0.0020
C18:1 CE	484470	1902412	3.92	0.0014
C20:4 CE	1120375	1306620	1.16	0.2274
C20:3 CE	74025	561756	7.58	0.0024
C22:6 CE	1032170	537918	0.521	8.852E-05

Table S2

Metabolite	*Mfds2a*$^{+/+}$ Average (Integrated Peak Area)	*Mfds2a*$^{-/-}$ Average (Integrated Peak Area)	Ratio *Mfds2a*$^{-/-}$: *Mfds2a*$^{+/+}$	p-value
C14:0 LPC	1330224	2197052	1.65	0.1627
C16:1 LPC	3220138	6365818	1.98	0.0730
C16:0 LPC	26145477	43343885	1.66	0.0897
C18:2 LPC	425827	880596	2.07	0.0748
C18:1 LPC	3960594	7476430	1.89	0.0783
C18:0 LPC	8812369	18102666	2.05	0.0507
C20:4 LPC	2130379	756938	0.36	0.0247
C20:3 LPC	10633863	17451766	1.64	0.0896
C16:0 LPE	1201757	2037139	1.70	0.1185
C18:1 LPE	603083	1831537	3.04	0.0371
C18:0 LPE	3267983	7004364	2.14	0.0683
C20:4 LPE	1370877	1073367	0.78	0.3590
C22:6 LPE	804230	102272	0.13	0.0031
C30:1 PC	90265643	143408710	1.59	0.2170
C30:0 PC	936244276	592579118	0.63	0.1027
C32:2 PC	104592527	212361050	2.03	0.0830
C32:1 PC	1911275661	2158082262	1.13	0.6311
C32:0 PC	2658033945	1392367536	0.52	0.0390
C34:4 PC	27374232	13477390	0.49	0.0429
C34:3 PC	55366198	88447735	1.60	0.2077
C34:2 PC	517305774	679238748	1.31	0.3559
C34:1 PC	3359088690	2760004311	0.82	0.3908
C34:0 PC	299918206	132498362	0.44	0.0328
C36:4 PC-B	656974220	233634591	0.36	0.0152
C36:3 PC	97795329	119219631	1.22	0.4864
C36:2 PC	300553113	400141984	1.33	0.3392
C36:1 PC	327027807	288625366	0.88	0.6204
C36:0 PC	1902725	1397648	0.73	0.2317
C38:6 PC	103893605	11023354	0.11	2.779E-05
C38:4 PC	380232424	132337164	0.35	0.0166
C38:3 PC	15418718	39800444	2.58	0.0562
C38:2 PC	7072704	14829304	2.10	0.0784
C40:10 PC	3916461	360331	0.09	0.0173
C40:9 PC	32662360	3730219	0.11	1.709E-05
C40:6 PC	55896708	5060988	0.09	0.0030
C34:4 PC-p	2407789	3130122	1.30	0.3655
C34:2 PC-p	2086377	2899887	1.39	0.2593
C34:1 PC-p -A	73855715	49800593	0.67	0.1543
C34:1 PC-p -B	302430	238548	0.79	0.0777
C36:5 PC-p -B	5552270	4483570	0.81	0.3116
C36:4 PC-p	20968745	15573031	0.74	0.2597
C36:2 PC-p	2075744	3436249	1.66	0.1405
C36:1 PC-p	1075310	1580765	1.47	0.2374
C38:4 PC-p	2855268	1096024	0.38	0.0656
C32:1 PE	5994315	13287823	2.22	0.0689
C32:0 PE	2743484	2410381	0.88	0.6550
C34:2 PE	12171881	40875031	3.36	0.0330
C34:0 PE	22145861	14772509	0.67	0.1219
C36:4 PE	68042811	61300894	0.90	0.6587
C36:3 PE	5895146	19241259	3.26	0.0321
C36:2 PE	20322779	55483850	2.73	0.0391
C36:1 PE	25891112	32412583	1.25	0.3967
C36:0 PE	7823210	4105286	0.52	0.0610

C38:6 PE	74736975	8820310	0.12	4.579E-06
C38:5 PE	43600839	64095330	1.47	0.1683
C38:4 PE	337152853	259117462	0.77	0.2515
C38:2 PE	12213932	10943860	0.90	0.7401
C40:6 PE	100291909	16062575	0.16	2.428E-05
C34:3 PE-p	2122354	14190828	6.69	0.0222
C34:2 PE-p	16680510	45429553	2.72	0.0342
C36:5 PE-p	50061359	39407443	0.79	0.2899
C36:4 PE-p	1768857	11443879	6.47	0.0205
C36:3 PE-p	3280143	23799411	7.26	0.0210
C36:2 PE-p	3009206	14581331	4.85	0.0206
C38:7 PE-p	55928379	9849964	0.18	0.0001
C38:6 PE-p	69059242	24522519	0.36	0.0692
C38:5 PE-p	38491795	26204547	0.68	0.1346
C40:7 PE-p	45364711	6182461	0.14	0.0003
C42:11 PE-p	2015869	593372	0.29	0.0021
C34:0 PI	22423018	7251128	0.32	0.0407
C36:4 PI	2385308	1512576	0.63	0.0640
C38:4 PI	15271396	9229568	0.60	0.0429
C36:1 PS	4321635	6646849	1.54	0.1495
C38:6 PS	3086186	2504173	0.81	0.2215
C38:4 PS	21194588	26018000	1.23	0.3402
C40:6 PS	37747957	10428366	0.28	0.0002
sphingosine	628998	715210	1.13	0.2480
C14:0 SM	263664	421698	1.59	0.2207
C16:1 SM	688187	742066	1.07	0.7613
C16:0 SM	23280304	25496216	1.09	0.6978
C18:1 SM	6926436	8195561	1.18	0.4917
C18:0 SM	68601927	72446204	1.05	0.8386
C20:0 SM	4190083	4176841	0.99	0.9916
C22:1 SM	484354	616350	1.27	0.4250
C22:0 SM	3221079	3245144	1.00	0.9761
C24:1 SM	6516459	8286961	1.27	0.3463
C24:0 SM	2312151	2177290	0.94	0.7789
C18:2 CE	161790	186657	1.15	0.5763
C20:5 CE	313142	199849	0.63	0.3034
C20:4 CE	378373	249975	0.66	0.1848

Table S4

A

Density of vesicular pits *in vitro*, Related to Figure 1						
Cell Source	**No. of experiments**	**No. of cell profiles**	**No. of pits/experiment**			**Mean vesicular pit density (/µm)**
bEnd.3 – mock infected	3	75 (25/experiment)	178	172	184	1.47 ± 0.24
bEnd.3 – Mfsd2a infected		75 (25/experiment)	99	76	63	0.64 ± 0.09
PANC-1 – GFP stably transfected	3	75 (25/experiment)	80	120	83	0.79 ± 0.01
PANC-1 – MFSD2A-GFP stably transfected		75 (25/experiment)	46	40	57	0.41 ± 0.05

B

Density of total membrane-connected vesicles in brain endothelial cells (P4), Related to Figure 3							
Genotype	**No. of animals**	**No. of endothelial cross-sections**	**No. of vesicles/animal**			**Luminal mean vesicular density (/µm)**	**Abluminal mean vesicular density (/µm)**
Mfsd2a$^{+/+}$	3	60 (20/animal)	81	63	78	0.33 ± 0.01	0.32 ± 0.01
Mfsd2a^{D96A}	3	60 (20/animal)	163	159	157	0.85 ± 0.03	0.79 ± 0.08

C

Density of Cav-1-positive vesicles in brain endothelial cells (P90), Related to Figure 5						
Genotype	**No. of animals**	**No. of endothelial cross-sections**	**No. of Cav-1 positive vesicles/animal**			**Mean vesicular density (/µm^2)**
Mfsd2a$^{+/+}$	3	30 (10/animal)	14	14	12	2.01 ± 0.14
Mfsd2a$^{-/-}$	3	30 (10/animal)	27	29	32	4.55 ± 0.81

D

Density of total membrane-connected vesicles in brain endothelial cells (P5), Related to Figure 6								
Genotype	**No. of animals**	**No. of endothelial cross-sections**	**No. of vesicles/animal**				**Luminal mean vesicular density (/µm)**	**Abluminal mean vesicular density (/µm)**
Mfsd2a$^{+/+}$; *Cav-1*$^{+/+}$	4	80 (20/animal)	81	83	74	81	0.34 ± 0.01	0.28 ± 0.02
Mfsd2a$^{-/-}$; *Cav-1*$^{+/+}$	4	80 (20/animal)	175	215	244	199	0.86 ± 0.08	0.86 ± 0.09
Mfsd2a$^{+/+}$; *Cav-1*$^{-/-}$	4	80 (20/animal)	42	35	49	35	0.17 ± 0.02	0.10 ± 0.01
Mfsd2a$^{-/-}$; *Cav-1*$^{-/-}$	4	80 (20/animal)	31	57	45	32	0.20 ± 0.03	0.09 ± 0.01

E

Density of clathrin-coated pits in brain endothelial cells (P5), Related to Figure S6								
Genotype	**No. of animals**	**No. of endothelial cross-sections**	**No. of vesicles/animal**				**Luminal mean vesicular density (/µm)**	**Abluminal mean vesicular density (/µm)**
Mfsd2a$^{+/+}$; *Cav-1*$^{+/+}$	4	80 (20/animal)	15	16	9	17	0.093 ± 0.01	0.017 ± 0.01
Mfsd2a$^{-/-}$; *Cav-1*$^{+/+}$	4	80 (20/animal)	14	11	12	17	0.096 ± 0.01	0.011 ± 0.01
Mfsd2a$^{+/+}$; *Cav-1*$^{-/-}$	4	80 (20/animal)	20	18	21	11	0.10 ± 0.02	0.018 ± 0.001
Mfsd2a$^{-/-}$; *Cav-1*$^{-/-}$	4	80 (20/animal)	9	38	22	11	0.12 ± 0.03	0.016 ± 0.014

F

Density of clathrin-coated pits in brain endothelial cells (P4), Related to Figure S6							
Genotype	**No. of animals**	**No. of endothelial cross-sections**	**No. of vesicles/animal**			**Luminal mean vesicular density (/µm)**	**Abluminal mean vesicular density (/µm)**
Mfsd2a$^{+/+}$	3	60 (20/animal)	16	15	13	0.098 ± 0.004	0.027 ± 0.007
Mfsd2a^{D96A}	3	60 (20/animal)	13	11	11	0.095 ± 0.02	0.034 ± 0.003

Supplemental Figure Legends

Figure S1. Validation of the transporter-dead *Mfsd2a*^{D96A} mutant mice. Related to Figure 2.

(A) PCR screening of *Mfsd2a*^{D96A} mice. A 250bp region spanning *Mfsd2a* exon 3 is amplified. Two additional silent mutations in codons 97/98 generate a SpeI restriction site, resulting in 100bp and 150bp fragments after digestion. Thus, *Mfsd2a*$^{+/+}$ mice produce one PCR fragment, with *Mfsd2a*$^{D96A/+}$ and *Mfsd2a*$^{D96A/D96A}$ mice producing three and two fragments, respectively. **(B-C)** Sanger sequencing of the D96A region in *Mfsd2a*$^{+/+}$ littermate controls (**B**) and *Mfsd2a*^{D96A} mutants (**C**). The purple and orange-boxed regions represent the D96A point mutation and new SpeI site, respectively. **(D-E)** Immunostaining at P4 of Mfsd2a protein (green) reveals vascular expression (purple, PECAM) in the cerebellum of both *Mfsd2a*$^{+/+}$ control **(D)** and *Mfsd2a*^{D96A} mutants **(E)**. *n* = 3 animals per genotype. Scale bar, 100 μm. **(F-G)** Immunostaining at P4 reveals absence of Mfsd2a protein expression in non-BBB-containing liver vasculature (purple, PECAM) of both *Mfsd2a*$^{+/+}$ control **(F)** and *Mfsd2a*^{D96A} mutants **(G)**. *n* = 3 animals per genotype. Scale bar, 100 μm.

Figure S2. Comprehensive lipidomic profiling of *Mfsd2a*^{D96A} and *Mfsd2a*$^{-/-}$ mutant brains. Related to Figure 2.

(A) Heatmap representation of the *Mfsd2a*^{D96A}-to-*Mfsd2a*$^{+/+}$ log-ratio of integrated mass spectrometry peak area for each phospholipid species analyzed. Brains were harvested from mutants and wild-type littermate controls at P4. *n* = 6 animals per genotype**. (B)** Heatmap representation of the *Mfsd2a*$^{-/-}$-to-*Mfsd2a*$^{+/+}$ log-ratio of integrated mass spectrometry peak area for each phospholipid species analyzed. Brains were harvested from mutants and wild-type littermate controls at P4. *n* = 4 animals per genotype. For all data, each species value is normalized to internal standard. (LPC, lyso-phosphatidylcholine; PC, phosphatidylcholine; LPE, lyso-phosphatidylethanolamine; PE, phosphatidylethanolamine; PS, phosphatidylserine; PI, phosphatidylinositol; p, plasmalogen).

Figure S3. *Mfsd2a*$^{-/-}$ and *Mfsd2a*^{D96A} mice display BBB leakage at adult stages and genetic inhibition of the caveolae pathway rescues BBB leakage defects in *Mfsd2a*$^{-/-}$ animals. Related to Figures 3 and 6.

(A-B) HRP tracer (dark brown) was injected into the circulation of *Mfsd2a*$^{+/+}$ **(A)** and *Mfsd2a*^{D96A} **(B)** mice at P90**.** Tracer diffuses into the forebrain parenchyma in *Mfsd2a*^{D96A} mutants (**B**), whereas tracer is confined to the vasculature in *Mfsd2a*$^{+/+}$ mice (**A**). *n* = 3 animals per genotype. Scale bar, 100 μm**. (C-F)** HRP tracer (dark brown) was injected into the circulation of *Mfsd2a*$^{+/+}$*; Cav-1*$^{+/+}$ **(C)**, *Mfsd2a*$^{-/-}$*; Cav-1*$^{+/+}$ **(D)**, *Mfsd2a*$^{+/+}$*; Cav-1*$^{-/-}$ **(E)**, and *Mfsd2a*$^{-/-}$*; Cav-1*$^{-/-}$ **(F)** mice at P90**.** Tracer diffuses into the forebrain parenchyma in *Mfsd2a*$^{-/-}$*; Cav-1*$^{+/+}$ single mutants (**D**), whereas tracer is confined to the vasculature in all other tested genotypes (**C,E, and F**). *n* = 4 animals per genotype. Scale bar, 100 μm**.**

Figure S4. Comprehensive lipidomic profiling of brain versus lung capillaries. Related to Figure 4.

(A) Western blot of NeuN (neuronal marker), VE-cadherin (endothelial cell marker), and β-Actin (loading control) proteins in acutely isolated capillaries from brains of P4 wild-type mice. Capillary lysates are free of neuronal contamination. **(B)** Western blot of VE-cadherin (endothelial cell marker), Pdgfr-β (pericyte marker), Aquaporin-4 (Aqp4, astrocyte endfeet marker), and β -Actin (loading control) proteins in acutely isolated capillaries and total tissue lysates from brains and lungs of wild-type mice. Both brain and lung capillary lysates are enriched in endothelial cells compared to total tissue lysates, and brain capillary lysates are free of astrocyte contamination. (**C**) Heatmap representation of the brain-to-lung log-ratio of integrated mass spectrometry peak area for each lipid species analyzed. Organs were harvested from wild-type mice at P4. Each species value is normalized to internal standard. (LPC, lyso-phosphatidylcholine; PC, phosphatidylcholine; LPE, lyso-phosphatidylethanolamine; PE, phosphatidylethanolamine; PS, phosphatidylserine; PI, phosphatidylinositol; p, plasmalogen; SM, sphingomyelin; CE, cholesteryl ester; MAG, monoacylglycerol; DAG, diacylglycerol; TAG, triacylglyceroyl). *n* = 6 groups per organ, 8 animals pooled per group.

Figure S5. Examples of lipid populations with higher levels in lung capillaries versus brain capillaries. Related to Figure 4.

(A) Lipidomic analysis of ethanolamine plasmalogen (PE-p) species from brain versus lung capillaries of P4 wild-type mice. **(B)** Lipidomic analysis of cholesteryl ester (CE) species from brain versus lung capillaries of P4 wild-type mice. **(C)** Lipidomic analysis of triacylglycerol (TAG) species from brain versus lung capillaries of P4 wild-type mice. For all data, value for each species is normalized to internal standard and expressed as brain-to-lung ratio of integrated mass spectrometry peak area. Data are mean ± s.e.m. For all data, n = 6 groups per organ, 8 animals pooled per group.

Figure S6. Clathrin-mediated pathway is not required for Mfsd2a regulation of BBB permeability. Related to Figures 3 and 6; Table S4.

(A) Example image of a clathrin-coated pit (CCP, red arrow) in CNS endothelial cells under electron microscopy. Scale bar, 100 nm. **(B-C)** Quantification shows no significant changes in clathrin-coated pit density along the luminal **(B)** or abluminal (**C**) plasma membrane in *Mfsd2a*$^{+/+}$*; Cav-1*$^{+/+}$*, Mfsd2a*$^{-/-}$*; Cav-1*$^{+/+}$*, Mfsd2a*$^{+/+}$*; Cav-1*$^{-/-}$, and *Mfsd2a*$^{-/-}$ *; Cav-1*$^{-/-}$ mice at P5. n = 4 animals per genotype, 20 capillary cross-sections per animal. **(D-E)** Quantification shows no significant changes in clathrin-coated pit density along the luminal **(D)** or abluminal (**E**) plasma membrane in *Mfsd2a*$^{+/+}$ and *Mfsd2a*^{D96A} mice at P4. n = 3 animals per genotype, 20 capillary cross-sections per animal. All data are mean ± s.e.m.; n.s., not significant.

Figure S7. Tight junctions are functional in CNS endothelial cells of *Cav-1*$^{-/-}$ mice. Related to Figure 6.

HRP tracer (black) fills the CNS vessel lumen (L) and enters intercellular clefts but is sharply halted at tight junction "kissing points" (yellow arrows) in both *Cav-1*$^{-/-}$ mutants (**C-D**) and *Cav-1*$^{+/+}$ littermate control animals (**A-B**) at P90. n = 3 animals per genotype. Scale bar, 100 nm.

Table S1. Lipidomic profiling of *Mfsd2a*^{D96A} mutant brains. Related to Figure 2.

Complete lipidomic analysis of phospholipid species from brain lysate of P4 *Mfsd2a*^{D96A} mutant and *Mfsd2a*$^{+/+}$ littermates (LPC, lyso-phosphatidylcholine; PC, phosphatidylcholine; LPE, lyso-phosphatidylethanolamine; PE, phosphatidylethanolamine; PS, phosphatidylserine; PI, phosphatidylinositol; p, plasmalogen; SM, sphingomyelin). Value for each species is normalized to internal standard and expressed as integrated mass spectrometry peak area. n = 6 animals per genotype.

Table S2. Lipidomic profiling of *Mfsd2a*$^{-/-}$ mutant brains. Related to Figure 2.

Complete lipidomic analysis of phospholipid species from brain lysate of P4 *Mfsd2a*$^{-/-}$ mutant and *Mfsd2a*$^{+/+}$ mice (LPC, lyso-phosphatidylcholine; PC, phosphatidylcholine; LPE, lyso-phosphatidylethanolamine; PE, phosphatidylethanolamine; PS, phosphatidylserine; PI, phosphatidylinositol; p, plasmalogen). Value for each species is normalized to internal standard and expressed at integrated mass spectrometry peak area. n = 4 animals per genotype.

Table S4. Quantification of EM images across multiple paradigms. Related to Figures 1, 3, 5, 6, and S5.

Raw quantification values of mean vesicular pit/vesicular density from all *in vitro* and *in vivo* experiments relating to Mfsd2a function. Density values were calculated from the number of vesicles per μm of membrane for each image collected. All images were collected at 12000x magnification. Density values for each cell source/genotype reflect the average of mean density values obtained from each individual experiment/animal and are expressed as mean ± s.e.m.

Data S1. Custom ImageJ macro for quantifying BBB tracer permeability assays. Related to STAR Methods.

```
//this macro quantifies the area of blood vessels and area of tracer in images from coronal forebrain sections after BBB tracer permeability assays

//initialize ImageJ
run("Colors...", "foreground=white background=black selection=yellow");
run("Options...", "iterations=1 count=1 black edm=Overwrite");
```

```
//choose folder with raw images and create folder to save processed images
rawdir=getDirectory("Choose Raw Data Folder");
resultdir=getDirectory("Choose Result Data Folder");
run("Set Measurements...", "area limit display redirect=None decimal=3");

//batch process raw images
var f;

list=getFileList(rawdir);
for(f=0;f<list.length;f++)
 {
  open(rawdir+list[f]);
  process();
 }

//measure area of vessels (C1) and tracer (C2)
function process()
 {
  //max z project
  //split channels and rename
  //run("Stack to Images");
  run("Z Project...", "projection=[Max Intensity]");
  run("Split Channels");
  //measure area of vessels
  selectWindow("C1-MAX_"+list[f]);run("Subtract Background...",
"rolling=70");setAutoThreshold("Huang dark");setOption("BlackBackground",
true);run("Convert to Mask");saveAs("Tiff",
resultdir+list[f]+"_vessels_Mask.tif");run("Analyze Particles...", "size=10-Infinity
display exclude summarize add");//saveAs("Tiff", resultdir+list[f]+"_vessels_Mask.tif");
  //measure area of tracer
  selectWindow("C2-MAX_"+list[f]);run("Subtract Background...",
"rolling=70");setAutoThreshold("Huang dark");setOption("BlackBackground",
true);run("Convert to Mask");saveAs("Tiff",
resultdir+list[f]+"_tracer_Mask.tif");run("Analyze Particles...", "size=10-Infinity display
exclude summarize add");//saveAs("Tiff", resultdir+list[f]+"_tracer_Mask.tif");

//save output as an Excel file
selectWindow("Summary");
saveAs("Text", resultdir+"Summary.xls");
run("Close All");
}
```